⌘ *Author's Choice*

THE JOURNAL OF BIOLOGICAL CHEMISTRY VOL. 283, NO. 45, pp. 31153–31162, November 7, 2008

Hypoxic Reactive Oxygen Species Regulate the Integrated Stress Response and Cell Survival*[S]

Received for publication, July 2, 2008, and in revised form, August 22, 2008 Published, JBC Papers in Press, September 3, 2008, DOI 10.1074/jbc.M805056200

Liping Liu[‡§], **David R. Wise**[§], **J. Alan Diehl**[§], **and M. Celeste Simon**[‡§1]

From the [‡]*Howard Hughes Medical Institute and* [§]*Abramson Family Cancer Research Institute, University of Pennsylvania School of Medicine, Philadelphia, Pennsylvania 19104*

Under hypoxic conditions, cells suppress energy-intensive mRNA translation by modulating the mammalian target of rapamycin (mTOR) and pancreatic eIF2α kinase (PERK) pathways. Much is known about hypoxic inhibition of mTOR activity; however, the cellular processes activating PERK remain unclear. Since hypoxia is known to increase intracellular reactive oxygen species (ROS), we hypothesized that hypoxic ROS regulate mTOR and PERK to control mRNA translation and cell survival. Our data indicate that although exogenous ROS inhibit mTOR, eIF2α, and eEF2, mTOR and eEF2 were largely refractory to ROS generated under moderate hypoxia (0.5% O_2). In direct contrast, the PERK/eIF2α/ATF4 integrated stress response (ISR) was activated by hypoxic ROS and contributed to global protein synthesis inhibition and adaptive ATF4-mediated gene expression. The ISR as well as exogenous growth factors were critical for cell viability during extended hypoxia, since ISR inhibition decreased the viability of cells deprived of O_2 and growth factors. Collectively, our data support an important role for ROS in hypoxic cell survival. Under conditions of moderate hypoxia, ROS induce the ISR, thereby promoting energy and redox homeostasis and enhancing cellular survival.

Hypoxia (O_2 deprivation) arises during embryonic development as well as pathophysiological conditions, such as tumor growth, tissue ischemia, stroke, and wound healing (1–3). Numerous studies indicate that O_2 availability regulates interdependent cell metabolism, growth, and survival (4–6). For example, cellular metabolism shifts from oxidative phosphorylation to anaerobic glycolysis under low O_2, partially mediated by stabilization of the α subunits of hypoxia-inducible factors (HIFs)[2] (4, 7, 8). HIF promotes glycolysis by inducing glucose transporters and glycolytic genes, such as phosphoglycerate kinase and lactate dehydrogenase A, and suppresses the tricarboxylic acid cycle via pyruvate dehydrogenase kinase 1 (9, 10). Additionally, hypoxia enhances O_2 delivery by activating genes involved in erythropoiesis and angiogenesis (2, 11). These adaptations contribute to O_2 and energy homeostasis. Nevertheless, chronic hypoxia markedly reduces intracellular ATP levels (12, 13). As an adaptive response, mRNA translation, ribosome biogenesis, and cell growth rates decrease during O_2 deprivation (13–15).

Hypoxia suppresses protein synthesis by inhibiting mRNA translation initiation and elongation (13, 16–18). Moderate hypoxia (0.5–1.5% O_2) inhibits m^7-GTP cap-dependent mRNA translation by rapid 4EBP1 hypophosphorylation. 4EBP1 is regulated in O_2-starved cells by inhibiting the mammalian target of rapamycin (mTOR), a key kinase promoting cell growth, metabolism, and proliferation. Hypoxia inhibits mTOR by 1) AMPK/TSC2 pathway activation upon energy depletion (13), 2) TSC2 stimulation by HIF-inducible REDD1 (15, 19, 20), and 3) promyelocytic leukemia-mediated mTOR nuclear translocation (21) (Fig. 1*A*). O_2 deprivation also causes eIF2α hyperphosphorylation by the endoplasmic reticulum (ER)-resident pancreatic eIF2α kinase (PERK) (Fig. 1*B*) (18, 22). These processes lead to a reduction in global protein synthesis. Finally, hypoxia increases eEF2 phosphorylation by eEF2 kinase, resulting in decreased translation elongation (Fig. 1*A*) (13, 23).

In contrast to global protein synthesis inhibition during hypoxia, translation of ATF4 (activating transcription factor 4) is enhanced upon PERK activation (Fig. 1*B*) (18, 24). ATF4 subsequently induces genes such as those encoding CHOP (DNA damage-inducible transcript 3), GADD34 (growth arrest and DNA-damage-inducible 34), and factors promoting glutathione biosynthesis and protein folding (Fig. 1*B*) (25, 26). Hypoxic PERK activation, eIF2α phosphorylation, and ATF4-mediated stress gene induction constitute a process known as the integrated stress response (ISR) (24, 27, 28), which is also activated by increased unfolded protein load in the ER, or by disrupting ER Ca^{2+} homeostasis (28, 29). GADD34, via complex formation with the catalytic subunit of protein phosphatase 1C, dephosphorylates eIF2α, forming a negative feedback loop to relieve hypoxic translational inhibition (Fig. 1*B*) (30). The ISR is an important protective response against anoxia; $PERK^{-/-}$ and eIF2α S51A mouse embryonic fibroblasts (MEFs) exhibit increased cell death when exposed to ≤0.02% O_2 (27). Furthermore, Ras-transformed $PERK^{-/-}$ MEFs form tumors more slowly and exhibit less angiogenesis than $PERK^{+/+}$ MEFs (22, 27).

Hypoxic mTOR regulation has attracted considerable attention, leading to the elucidation of multiple underlying mecha-

* This work was supported, in whole or in part, by National Institutes of Health Grant PO1 CA 104838. This work was also supported by the Abramson Family Cancer Research Institute. The costs of publication of this article were defrayed in part by the payment of page charges. This article must therefore be hereby marked "*advertisement*" in accordance with 18 U.S.C. Section 1734 solely to indicate this fact.

⌘ *Author's Choice*—Final version full access.

[S] The on-line version of this article (available at http://www.jbc.org) contains supplemental Figs. 1–3.

[1] An investigator of the Howard Hughes Medical Institute. To whom correspondence should be addressed: 421 Curie Blvd., Philadelphia, PA 19104. Tel.: 215-746-5532; Fax: 215-746-5511; E-mail: celeste2@mail.med.upenn.edu.

[2] The abbreviations used are: HIF, hypoxia-inducible factor; mTOR, mammalian target of rapamycin; ER, endoplasmic reticulum; PERK, pancreatic eIF2α kinase; ISR, integrated stress response; MEF, mouse embryo fibroblast; TNFα, tumor necrosis factor α; mtROS, mitochondrial ROS; PKR, RNA-activated protein kinase; FBS, fetal bovine serum; GFP, green fluorescent protein; BME, β-mecaptoethanol; DKO, double knock-out; TKO, triple knock-out; EC, embryonic cell.

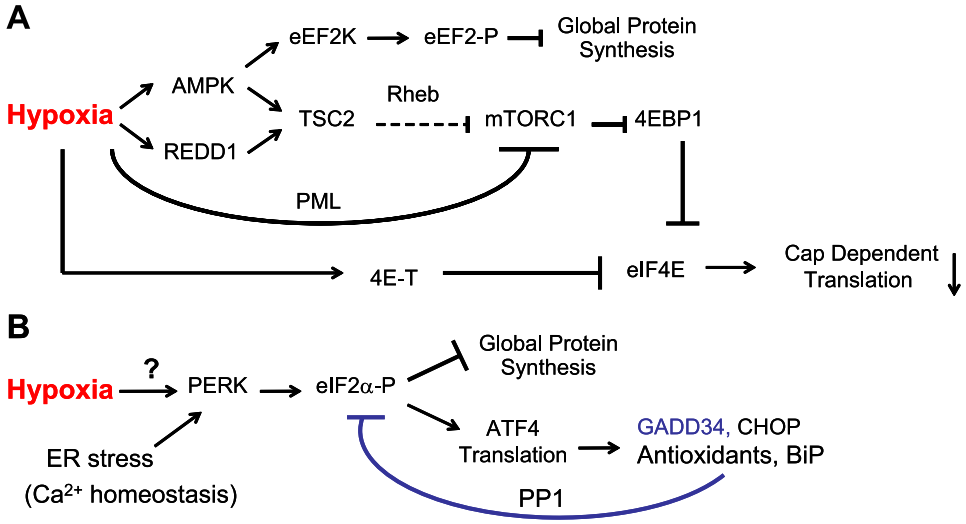

FIGURE 1. **Hypoxia inhibits multiple pathways regulating mRNA translation.** *A* and *B*, schematic diagram of signaling pathways regulating mRNA translation during hypoxia. These include the regulation of translation elongation and availability of eIF4E protein by modulating 4EBP1 phosphorylation (*A*) and eIF2α phosphorylation (*B*). *A*, hypoxia inhibits cap-dependent translation via activating the AMPK/TSC2 and REDD1/TSC2 pathways and promyelocytic leukemia-mediated mTOR nuclear translocation. eIF4E is also regulated by 4E-T sequestration in hypoxic cells. Furthermore, AMPK phosphorylates eEF2 kinase (eEF2K), leading to eEF2 phosphorylation and the inhibition of translation elongation and global protein synthesis. *B*, hypoxia also inhibits global protein synthesis by PERK-mediated eIF2α phosphorylation. Other stresses (*e.g.* increased protein load or disruption of protein glycosylation in the ER) and perturbations in Ca^{2+} homeostasis also result in PERK activation. The ATF4/GADD34/eIF2α negative feedback loop relieves translational inhibition.

nisms. In contrast, molecular events resulting in an ISR within hypoxic cells have not been fully delineated. Additionally, mechanism(s) responsible for the rapid HIF- and AMPK-independent mTOR inhibition observed within 30 min of hypoxia remain unclear (13, 15, 31). We hypothesized that enhanced reactive oxygen species (ROS) generation during hypoxia could mediate PERK and mTOR regulation. Several reports indicate that ROS can inhibit pathways regulating mRNA translation (32–34). For example, H_2O_2 causes 4EBP1 hypophosphorylation (33), and oxidative stress stimulated by arsenate and TNFα leads to eIF2α phosphorylation (34, 35). In mammalian cells, ROS are formed in response to toxic reagents or as by-products of O_2-utilizing cellular processes, such as mitochondrial electron transport, cytochrome P450 enzymatic activity, or NADH/NADPH oxidation (36, 37). ROS have been shown to act as signaling molecules, activating ASK1 (apoptosis signal-regulated kinase 1) and oxidizing reactive cysteine residues in protein-tyrosine phosphatases and protein kinase C (36–38).

Hypoxia increases intracellular ROS production in a variety of cells (39–41). Mitochondria appear to be the primary source for ROS during hypoxia, and mitochondrial ROS (mtROS) are sufficient to stimulate multiple biological responses during O_2 deprivation (40–43). Enzymatic antioxidants, such as catalase and glutathione peroxidase, suppress HIF-1α accumulation during O_2 deprivation (40, 42), suggesting that H_2O_2 is a key biologically active form of ROS during hypoxia. We investigated the role of increased oxidative stress in regulating the ISR and mTOR and consequent effects on mRNA translation during O_2 deprivation. We also examined signaling pathways activated by exogenous ROS that exert translational regulation and compared these with hypoxia. We demonstrate that exogenous ROS regulate mTOR by a TSC2-independent mechanism and induce eIF2α phosphorylation by multiple kinases, including PERK and interferon-induced, double-stranded RNA-activated protein kinase (PKR). More importantly, we report that although endogenous ROS do not regulate mTOR and eEF2, increased mtROS are critical for ISR activation during hypoxia. This ROS-induced ISR promotes energy and redox homeostasis by modulating protein synthesis and the induction of ATF4 target genes and constitutes an important early adaptive response to enhance cell survival and hypoxia tolerance.

EXPERIMENTAL PROCEDURES

Materials—Antibodies for eIF2α and 4EBP1 proteins, phospho-eIF2α, rpS6, and AMPK were obtained from Cell Signaling Technology. Antibody for PERK was kindly provided by Dr. J. A. Diehl (University of Pennsylvania). Antibodies for ATF4, GADD34, and CHOP were purchased from Santa Cruz Biotechnology, Inc. (Santa Cruz, CA). Insulin, H_2O_2, uridine, *N*-acetyl cysteine, and thapsigargin were from Sigma. Dulbecco's modified Eagle's medium (glucose-free) was purchased from Invitrogen. Recombinant mouse TNFα was purchased from Cell Sciences. [^{35}S]Methionine was obtained from Amersham Biosciences.

Cell Culture—Wild-type, $PERK^{-/-}$, $PERK^{-/-}/GCN2^{-/-}$ (double knock-out (DKO)), and $PERK^{-/-}/GCN2^{-/-}/PKR^{-/-}$ (triple knock-out (TKO)) MEFs were kind gifts from Dr. D. Cavener (Pennsylvania State University) (25). The MEFs carrying knock-in mutations of either eIF2α S51S or S51A were kindly provided by Dr. R. Kaufman (44). $TSC2^{-/-}/p53^{-/-}$ and $TSC2^{+/+}/p53^{-/-}$ MEFs were gifts from Dr. D. Kwiatkowski (Harvard University) (13). HEK293 cells and MEFs were propagated in Dulbecco's modified Eagle's medium supplemented with 10% fetal bovine serum (FBS) (Gemini Bioproducts) and 4.5 g/liter glucose, as described previously (13). 55 μM β-mercaptoethanol (BME) was included during passage for various MEFs. Cytochrome *c* wild type and null embryonic cells were derived and cultured as described previously (41).

Cells were plated at varying densities to achieve ~60–80% confluence at the end of treatments. The cells were shifted to BME-free medium and allowed to adhere for 16 h before any treatment. Hypoxia was generated using an $InVivo_2$ 400 hypoxic work station (Biotrace). Alternatively, cells were exposed to H_2O_2 for 1 h (replenished every 30 min) or 0.8 μM thapsigargin for 4 h. One set of cells was pretreated with either 100 μM BME or 5 mM *N*-acetyl cysteine 2 h before exposure to low O_2 or H_2O_2.

Expression Constructs and Transfection—The pCMVSport6-catalase (mouse) plasmid was purchased from Open Biosystems. HEK293 cells were transfected using Lipofectamine 2000 (Invitrogen) and allowed 48 h for catalase expression. Catalase-

and GFP-expressing adenoviruses were obtained from the Gene Transfer Vector Core (University of Iowa) and Baylor College of Medicine Vector Development Laboratory, respectively (40). MEFs were transduced (500 plaque-forming units/cell) and allowed 30 h for expression.

Western and Protein Carbonylation Analysis—All cultures were harvested under either normoxia or hypoxia, and Western blotting was performed as described previously (13, 31). Protein carbonylation in cell lysates was detected using an OxyBlot™ protein oxidation detection kit (Chemicon).

Quantitative Real Time PCR—Total RNA was isolated using TRIzol (Invitrogen). First strand cDNA was synthesized using 2 μg of RNA, random hexamers, and the Superscript II First-Strand Synthesis System for RT-PCR (Invitrogen). Quantitative real time PCR was performed using the Applied Biosystems 7900HT Sequence Detection System and SyberGreen PCR Master Mix (Applied Biosystems). All primers were generated using PrimerExpress1.0 software (sequence available upon request). β-Actin was used for endogenous control in $\Delta\Delta CT$ analysis.

^{35}S-Protein Synthesis—Cells seeded in 12-well plates were subjected to 48 h of 0.5% O_2 or 1 h of H_2O_2 (20 or 100 μM). Cells were labeled with [^{35}S]methionine for 1 h under low O_2 or H_2O_2. Radioactivity in cell lysates was determined as described previously (13) and adjusted with protein content in each sample.

ATP Measurement—The eIF2α S51S and S51A MEFs (1000 cells/well in 96-well plates) were exposed to 21% or 0.5% O_2 for 48 h in medium similarly to colony formation assays. Cellular ATP levels were examined using the ApoGlow assay kit (Lonza). The data were expressed as percentiles of normoxic cells grown in the same medium.

Colony Formation Assay—S51A and S51A MEFs were plated at 1000 cells/well in a 6-well plate and allowed to adhere overnight before 2 h of pretreatment with 5 mM *N*-acetyl cysteine or drug vehicle. The cells were then exposed to 21 or 0.5% O_2 for 24 or 48 h in Dulbecco's modified Eagle's medium consisting of full serum and glucose (10% FBS, 4.5 g/liter glucose), medium deprived of serum (0.5% FBS, 4.5 g/liter glucose) or medium deprived of glucose (10% FBS, 0.2 g/liter glucose). The cells were shifted back to regular medium and grown for 1 week under normoxia. Colonies were stained using 0.4% crystal violet and counted.

Statistical Analysis—Results are average ± S.E. of 4–6 samples from two independent studies. Statistical analyses were performed using two-tailed Student's *t* test. *Error bars* represent S.E. for all figures. Statistical significance was defined as follows: *, #, or ◇, $p < 0.05$; ** or ##, $p < 0.01$.

RESULTS

Hypoxia Inhibits Signaling Pathways Regulating mRNA Translation—Among the four mammalian eIF2α kinases (PERK, GCN2 (GCN2 eIF2α kinase), PKR, and heme-regulated initiation factor 2-α kinase (HRI)), PERK appears to be the principal regulator of eIF2 when O_2 levels are ≤0.02% O_2 (18). Since modest hypoxia (>0.2% O_2) and anoxia (≤0.02% O_2) exhibit different kinetics of 4EBP1 and eIF2α regulation (13, 46, 47), we examined the effects of PERK on eIF2α during moderate hypoxia (0.5% O_2). Phosphorylation of eIF2α on Ser^{51} increased

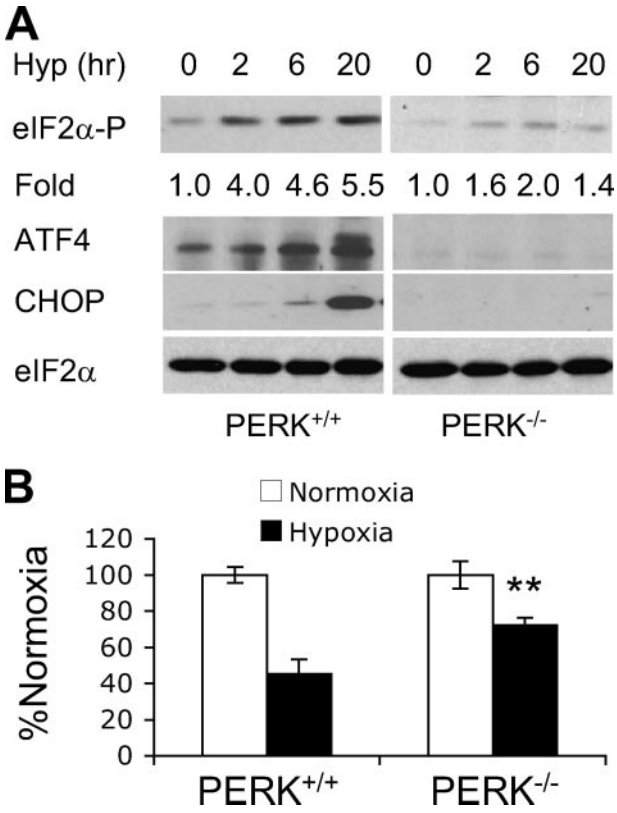

FIGURE 2. **PERK is required for induction of the integrated stress response and protein synthesis inhibition during hypoxia.** *A*, eIF2α phosphorylation in PERK$^{+/+}$ and PERK$^{-/-}$ MEFs exposed to 0–20 h 0.5% O_2. Quantitative changes in eIF2α phosphorylation, compared with 0 h hypoxia based on Image J analysis, are indicated. Total eIF2α protein serves as a loading control. Also shown is the accumulation of ATF4 and CHOP proteins in PERK$^{+/+}$ and PERK$^{-/-}$ MEFs. *B*, protein synthesis in MEFs after 48 h 0.5% O_2 measured by [^{35}S]methionine incorporation. See "Experimental Procedures" for statistical analyses. **, $p < 0.01$.

4-fold in PERK$^{+/+}$ MEFs after 2 h and was maintained over 20 h (Fig. 2*A*). In contrast, eIF2α phosphorylation was only increased 2-fold in PERK$^{-/-}$ MEFs (Fig. 1*C*). Therefore, PERK is the principal eIF2α kinase operating under moderate hypoxia, although other kinases contribute to eIF2α inhibition. Of note, all Western blot assays depicted in Figs. 2–7 were repeated 3–5 times to allow precise quantitation of phosphorylation changes. PERK was also required for the induction of ATF4 and CHOP in O_2-deprived cells (Fig. 2*A*). Finally, hypoxic PERK activation correlated with a significant drop in protein synthesis, as measured by [^{35}S]methionine pulse labeling. Exposure of serum-replete MEFs to 0.5% O_2 for 48 h resulted in a 55% drop in metabolic labeling (Fig. 2*B*). PERK deletion restored translation rates to ~70%, further indicating that PERK is critical for translational inhibition during chronic but moderate hypoxia.

ROS Inhibit Signaling for mRNA Translation—To investigate whether increased ROS levels mediate hypoxic regulation of mRNA translation, we characterized the effects of ROS on signaling pathways controlling protein synthesis. We employed MEFs and HEK293 cells for these studies, since both have been used extensively for the evaluation of mTOR and the ISR (13, 15, 18, 19). Initially, we treated cells with exogenous H_2O_2, the major form of intracellular ROS generated during O_2 deprivation (40, 42). Higher

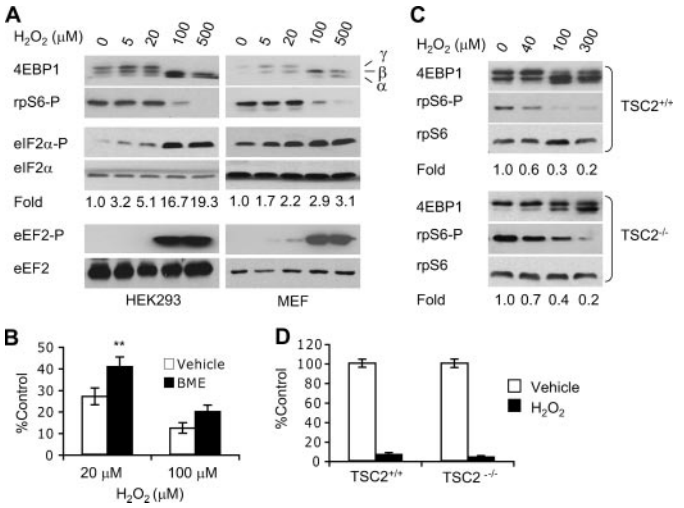

FIGURE 3. **Effects of H_2O_2 on mRNA translation and protein synthesis.** *A*, HEK293 cells and immortalized wild-type mouse embryonic fibroblasts (MEFs) were exposed to 0–500 μM H_2O_2 for 1 h. Whole cell extracts were blotted for 4EBP1, phospho-rpS6, phospho-eIF2α, total eIF2α, phospho-eEF2, and total eEF2. Hypophosphorylated (α) and phosphorylated (β and γ) forms of 4EBP1 are indicated. Levels of total eIF2α and eEF2 proteins were examined for sample loading and protein stability using the same lysates run on separate gels. Changes in eIF2α phosphorylation (based on Image J analysis) compared with 0 μM H_2O_2 are shown. *B*, protein synthesis in H_2O_2-treated (1 h) MEFs with or without 2 h BME (100 μM) preconditioning. BME (100 μM) was present during the 1-h protein synthesis. **, $p < 0.01$. *C*, Western blotting for total 4EBP1 protein and rpS6 phospho-$Ser^{235/236}$ in H_2O_2-treated (1 h) $TSC2^{+/+}$ and $TSC2^{-/-}$ MEFs. Changes in rpS6 phosphorylation compared with 0 μM H_2O_2 are indicated. *D*, protein synthesis in $TSC2^{+/+}$ and $TSC2^{-/-}$ MEFs treated with 100 μM H_2O_2 (1 h). [^{35}S]Methionine labeling was carried out in the presence of 100 μM H_2O_2. Base-line protein synthesis was similar in $TSC2^{+/+}$ and $TSC2^{-/-}$ cells.

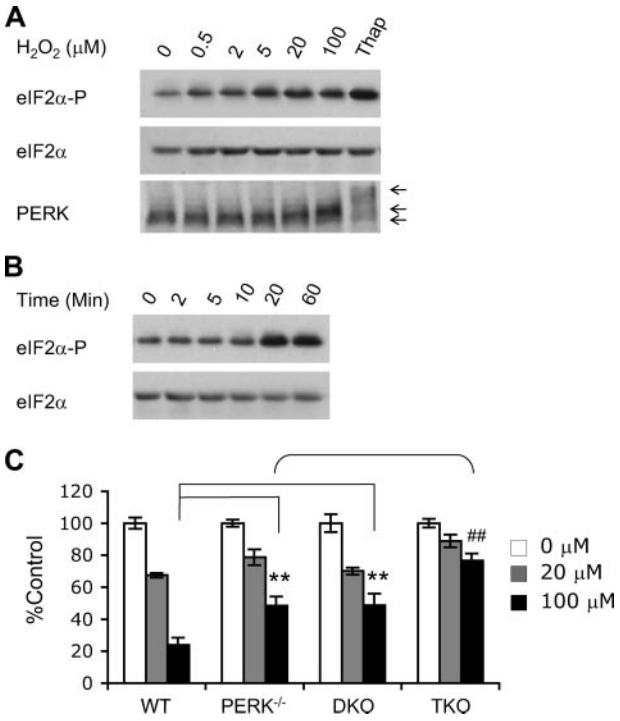

FIGURE 4. **Role of eIF2α kinases in H_2O_2-induced eIF2α phosphorylation.** *A*, HEK293 cells were exposed to varying concentrations of H_2O_2 (1 h) or 0.8 μM thapsigargin (4 h). Cell lysates were probed for phospho-eIF2α, total eIF2α, and PERK. The *arrows* indicate mobility changes for PERK proteins. *B*, eIF2α phosphorylation in HEK293 cells exposed to 20 μM H_2O_2 for 0–60 min. *C*, protein synthesis in MEFs treated with 0–100 μM H_2O_2 (1 h) ($n = 9$–10). **, $p < 0.01$; wild-type (*WT*) *versus* $PERK^{-/-}$ or DKO ($PERK^{-/-}$, $GCN2^{-/-}$) MEFs subjected to 100 μM H_2O_2. ##, $p < 0.01$; TKO ($PERK^{-/-}$, $GCN2^{-/-}$, $PKR^{-/-}$) MEFs showed significantly higher protein synthesis in comparison with $PERK^{-/-}$ and DKO MEFs upon exposure to 100 μM H_2O_2.

H_2O_2 doses (100–500 μM, 1 h) significantly inhibited mTOR in HEK293 cells and MEFs based on 4EBP1 and rpS6 hypophosphorylation (Fig. 3*A*). However, lower H_2O_2 doses (5–20 μM) did not appreciably affect mTOR activity. Moreover, H_2O_2 inhibited translation elongation with a dose response similar to mTOR. High H_2O_2 concentrations (100–500 μM) caused significant eEF2 phosphorylation (Fig. 3*A*), whereas low H_2O_2 doses (5–20 μM) did not. In direct contrast, eIF2α phosphorylation was triggered by as low as 5 μM H_2O_2 (Fig. 3*A*) and enhanced by increasing H_2O_2 concentrations.

Repression of eIF4E, eIF2, and eEF2 activities correlated with a significant drop in protein synthesis. As shown in Fig. 3*B*, 20–100 μM H_2O_2 for 1 h inhibited protein synthesis 70–90%, respectively, in MEFs. Furthermore, the antioxidant BME partially blocked the reduction in protein synthesis caused by H_2O_2 (Fig. 3*B*). To investigate whether attenuated signaling and protein synthesis is a direct consequence of cell death, we assessed the effects of H_2O_2 on cell viability using trypan blue staining. Of note, ~90% of cells were viable immediately following treatment with 100 μM H_2O_2 for 1 h (supplemental Fig. 1*A*), indicating that mRNA translation inhibition did not result from acute cell death. Together, these data indicate that ROS inhibit mRNA translation and that eIF2α phosphorylation is significantly more sensitive to oxidative stress than mTOR regulation or eEF2 phosphorylation.

TSC2 Is Not Required for mTOR Inhibition by Peroxide—TSC2 is necessary for acute hypoxic mTOR inhibition (13, 19). Therefore, we determined if TSC2 is required for mTOR regulation by H_2O_2. As shown in Fig. 3*C*, $TSC2^{-/-}$ MEFs exhibited a higher basal level of mTOR activity in comparison with $TSC2^{+/+}$ MEFs (indicated by 4EBP1 and rpS6 hyperphosphorylation). H_2O_2 (40–300 μM) gradually suppressed mTOR activity in both cell types, regardless of TSC2 status (Fig. 3*C*). We concluded that TSC2 is dispensable for mTOR inactivation by H_2O_2. Furthermore, H_2O_2 (100 μM) inhibited protein synthesis by 90% in both $TSC2^{+/+}$ and $TSC2^{-/-}$ cells (Fig. 3*D*), confirming that TSC2 is not essential for mTOR regulation by oxidative stress. Because TSC2 is required for rapid mTOR inhibition by hypoxia (13, 15, 19), the data indicate that acute hypoxic mTOR regulation is unlikely to involve H_2O_2.

eIF2α Kinases and H_2O_2-induced eIF2α Phosphorylation—PERK is critical for hypoxic eIF2α phosphorylation (see Fig. 2*A*). We therefore investigated whether PERK plays a role in eIF2α regulation during oxidative stress. $PERK^{+/+}$ MEFs were exposed to 0–100 μM H_2O_2 for 1 h, and eIF2α phosphorylation and PERK protein mobility (an assay typically used to study PERK activation (28, 34)) were examined by Western blots. As little as 0.5 μM H_2O_2 elevated eIF2α phosphorylation, which was enhanced as H_2O_2 concentration increased to 100 μM (Fig. 4*A*), demonstrating that eIF2α is readily inhibited by oxidative stress. A time course study using 20 μM H_2O_2 showed significantly increased eIF2α phosphorylation after a 20-min exposure (Fig. 4*B*), demonstrating rapid kinetics for eIF2 inhibition by oxidative stress. Importantly, H_2O_2 (20 and 100 μM) also caused a moderate but reproducibly detectable shift in PERK

protein mobility (Fig. 4*A*), suggesting a dose-dependent post-translational modification of PERK proteins caused by H_2O_2. High H_2O_2 levels resulted in increased PERK protein modification, resolved from unmodified PERK by a slight mobility shift. However, H_2O_2-induced PERK mobility change was significantly less pronounced than that resulting from thapsigargin, an ionophore disrupting ER Ca^{2+} stores. The reason(s) for this distinction are unclear at this time.

The multifactorial involvement of eIF2α kinases in H_2O_2 responses was supported by examining protein synthesis using mutant MEFs. As shown in Fig. 4*C*, 100 μM H_2O_2 caused a 75% reduction in metabolic ^{35}S labeling in wild-type MEFs, whereas both $PERK^{-/-}$ and $PERK^{-/-}$ $GCN2^{-/-}$ DKO cells exhibited 50% inhibition of mRNA translation. PKR deletion in addition to PERK and GCN2 in TKO cells further alleviated the inhibition to 25% of vehicle control. Thus, we concluded that ROS activate multiple eIF2α kinases, including PERK and PKR. However, GCN2 does not appear to play a major role in this pathway.

Hypoxia Enhances ROS Release—We evaluated the impact of endogenous cellular ROS generated at 0.5% O_2 on pathways regulating mRNA translation. Given difficulties with typical 2′,7′-dichlorofluorescein diacetate assays of O_2-deprived cells (40), we tested protein carbonylation as an indicator of oxidative stress. In this assay, whole cell lysates are probed to reveal multiple polypeptides exhibiting carbonyl modifications. Here, HEK293 cells were treated with H_2O_2, hypoxia, or TNFα for varying lengths of time. H_2O_2 (20 μM, 1 h) resulted in modest protein carbonylation (Fig. 5*A*), whereas 100 μM H_2O_2 (1 h) generated significant protein carbonylation (Fig. 5*A*). As shown in supplemental Fig. 2, treatment of cells with 100 μM H_2O_2 is roughly comparable with growth in 0.5% O_2 based on 2′,7′-dichlorofluorescein diacetate fluorescence (although this assay is imperfect). Hypoxia for 2 h caused modest but reproducibly detectable increases in protein carbonylation, which was enhanced by extending treatment to 20 h (Fig. 5*A*). Of note, TNFα, a cytokine augmenting intracellular ROS (34), and 0.5% O_2 (20 h) resulted in similar levels of protein carbonylation. Therefore, oxidative damage accumulates during hypoxia. Furthermore, O_2 deprivation results in intracellular ROS levels comparable with or slightly less than TNFα treatment and 100 μM H_2O_2.

Effects of hypoxic ROS on PERK activation were examined by measuring PERK protein mobility. Hypoxia (8–24 h) reproducibly induced subtle reductions in PERK mobility. Importantly, hypoxic alteration of PERK mobility was comparable with that of peroxide (20–100 μM) (Fig. 5*B*). High doses (100 μM) caused enhanced PERK modification and increased resolution from unmodified PERK protein (Fig. 5*B* and supplemental Fig. 1*B*). Mobility changes induced by hypoxia and H_2O_2 were significantly less than that caused by thapsigargin (Fig. 5*B*). As stated above, the reasons for these distinct effects on PERK mobility are currently unknown.

Hypoxic mTOR Regulation Does Not Involve ROS—To examine whether hypoxic mTOR inactivation is mediated by ROS, MEFs were infected with adenoviral catalase or GFP (negative control) and exposed to 0.5% O_2 or H_2O_2. Catalase blocked H_2O_2-induced p70S6K and 4EBP1 hypophosphorylation, demonstrating that catalase is capable of effectively scavenging H_2O_2 in MEFs (Fig. 5*C*). Of note, hypoxic p70S6K and 4EBP1 hypophosphorylation was not affected by catalase expression (Fig. 5*C*), implying that hypoxic mTOR regulation is independent of redox change.

To further evaluate ROS involvement in hypoxic mTOR and eEF2 regulation, HEK293 cells were transfected with empty vector or plasmid encoding catalase. As shown in Fig. 5*D*, expression of catalase effectively alleviated H_2O_2-induced rpS6 hypophosphorylation but not rpS6 hypophosphorylation caused by 20-h hypoxia, confirming that ROS do not affect mTOR activity during hypoxia. Similar to rpS6, catalase had an insignificant effect on eEF2 phosphorylation during hypoxia (Fig. 5*D*). Collectively, these data demonstrate that although ROS suppress mTOR and eEF2 activities *in vitro*, hypoxic mTOR and eEF2 inhibition does not involve ROS.

ROS Activate the ISR during Hypoxia—Given the similarity of hypoxia and H_2O_2 in causing subtle PERK mobility changes, we studied the effects of oxidative stress on PERK activation during hypoxia. Of note, eIF2α phosphorylation caused by hypoxia (20 h) and peroxide (20 μM) was reduced by catalase (Fig. 5*D*), implying that increased H_2O_2 during hypoxia activates the PERK/eIF2α pathway. To extend these data, we tested hypoxic induction of ATF4 target genes in HEK293 cells using quantitative real time PCR. Hypoxia treatment induced GADD34, BiP, and CHOP as well as the HIF target phosphoglycerate kinase (Fig. 4*E*). Although catalase only partially reduced phosphoglycerate kinase induction (Fig. 5*E*), it effectively blocked the induction of all three ER stress genes during hypoxia (Fig. 5*E*), supporting the conclusion that enhanced ROS induce the ISR. Similarly, H_2O_2 (20 μM, 6 h) dramatically increased GADD34, BiP, and CHOP expression in HEK293 cells, which was repressed by catalase (supplemental Fig. 3*A*). Interestingly, H_2O_2 moderately enhanced phosphoglycerate kinase expression, and phosphoglycerate kinase induction was also suppressed by catalase (supplemental Fig. 3*B*). H_2O_2-induced phosphoglycerate kinase probably results from ROS-mediated HIF-1α protein accumulation (40–42). Overall, our data demonstrate that ROS and hypoxia activate the ISR, and these responses are abrogated by ROS scavengers.

We next determined whether catalase blockade of eIF2α phosphorylation affects actual protein synthesis during O_2 deprivation. This was accomplished using MEFs infected with adenoviral GFP or catalase. As shown in Fig. 5*F*, catalase attenuated hypoxia-induced decreases in metabolic labeling from 45 to 25%, verifying that ROS play a partial role in regulating mRNA translation during hypoxia. The remaining 25% reduction in protein synthesis probably results from ROS-independent 4EBP1, eIF4E, and eEF2 modulation. In summary, we concluded that oxidative stress during hypoxia induces the ISR, resulting in decreased protein synthesis and activation of ATF4-regulated stress genes. Importantly, peroxide scavengers effectively suppress these stress responses.

Mitochondrial ROS Modulate eIF2 Activity during Hypoxia—Because ROS are important for activating the ISR during hypoxia, we investigated the source(s) of ROS causing this effect. ROS are produced by various cellular processes and organelles, including mitochondria and the ER (26, 48, 49). ER ROS are largely

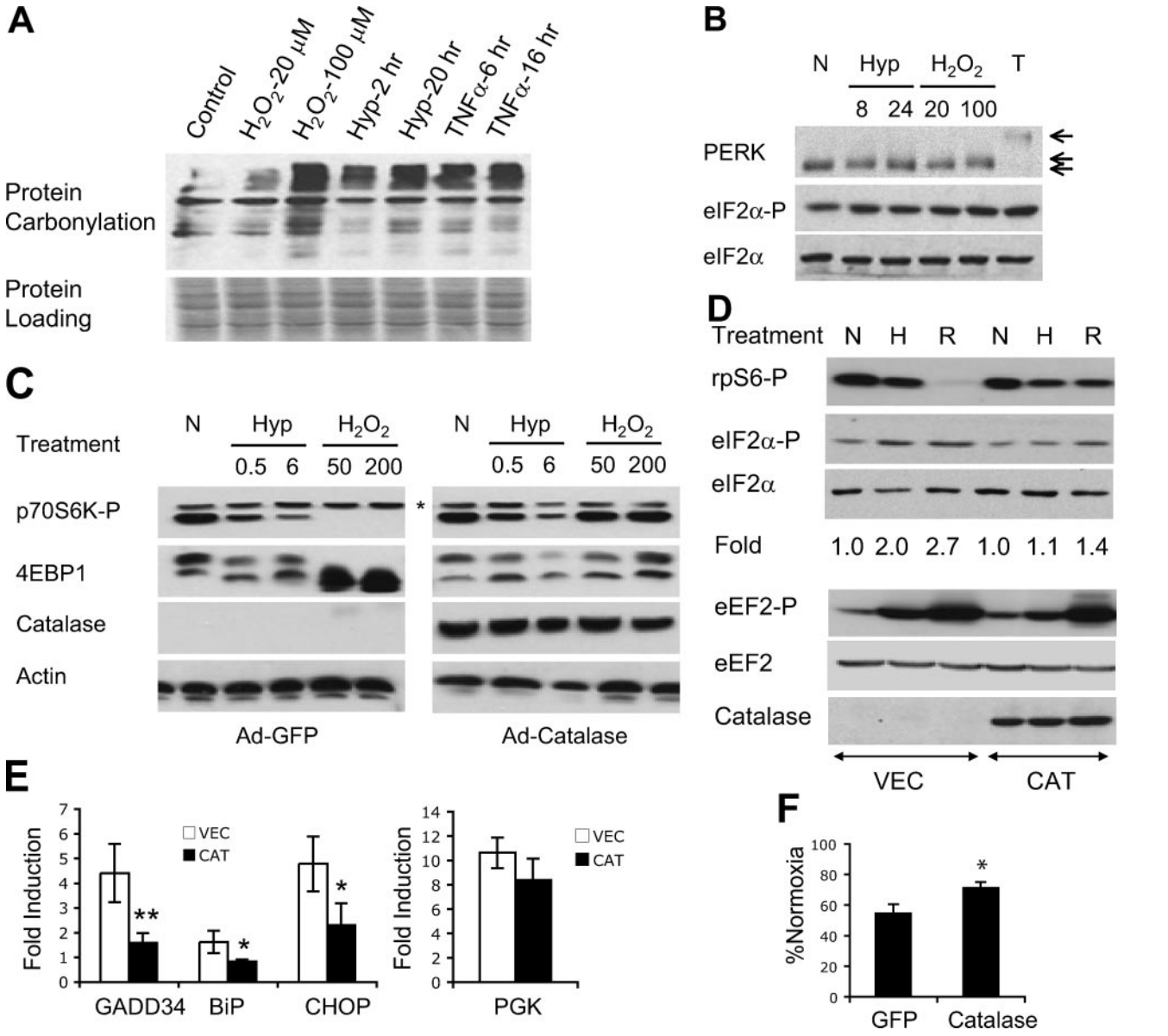

FIGURE 5. **Role of ROS during hypoxic regulation of mRNA translation.** *A*, HEK293 cells were exposed to H_2O (vehicle control), H_2O_2 (20 or 100 μM, 1 h), hypoxia (*Hyp*; 0.5% O_2, 2 or 20 h), or TNFα (10 ng/ml, 6 or 16 h). Protein carbonylation in whole cell extracts was examined. Equivalent sample loading was based on Ponceau staining. *B*, HEK293 cells were exposed to hypoxia (0.5% O_2, 8 or 24 h), H_2O_2 (20 or 100 μM, 1 h), or thapsigargin (*T*) (0.8 μM, 4 h). Mobility of total PERK proteins and phosphorylation of eIF2α were determined. *C*, MEFs infected with adenoviral GFP or catalase were exposed to hypoxia (0.5% O_2, 0.5 or 6 h) or H_2O_2 (50 or 200 μM, 1 h). Phosphorylation of p70S6K and 4EBP1 was examined using anti-phospho-p70S6K (Thr^{389}) and total 4EBP1 antibodies. *, the p80S6K isoform, which did not change appreciably during any treatments. The status of 4EBP1 is indicated by mobility shift from phosphorylated β form to hypophosphorylated α form. *D*, HEK293 cells transfected with catalase or empty vector were exposed to 21% (*N*) or 0.5% O_2 (*H*) for 20 h, or 50 μM H_2O_2 for 1 h (*R*). Phosphorylation of rpS6, eIF2α, and eEF2 proteins was determined. Quantitative changes in eIF2α phosphorylation are shown. *E*, expression of mRNA for GADD34, BiP, CHOP, and phosphoglycerate kinase in HEK293 cells transfected with catalase (*CAT*) or vector (*VEC*) following 20 h of 21% or 0.5% O_2. *F*, protein synthesis in adenoviral GFP- or catalase-expressing MEFs after 48 h 0.5% O_2. *, $p < 0.05$; **, $p < 0.01$.

generated by ERO1 (endoplasmic reticulum oxidase-1) to facilitate intramolecular disulfide bond formation and protein folding (49). Marciniak *et al.* (50) previously demonstrated that neither ERO1 RNA interference nor stable interfering ERO1 transgenes reproducibly affected ER redox in mammalian cells. Consequently, we did not attempt to modulate ER redox in our assays. Instead, we investigated the effects of mtROS on the ISR and mRNA translation under O_2 deprivation given that mtROS are biologically active (40, 41). Loss of cytochrome *c*, a key component of the mitochondrial electron transport chain, greatly diminishes mtROS release during hypoxia (41). Therefore, we employed wild type and cytochrome *c*-null embryonic cells (ECs) in our studies.

ECs were exposed to 0.5% O_2 for 0–12 h. HIF accumulation and phosphorylation of eIF2α and the mTOR downstream targets rpS6 and 4EBP1 were examined. Cytochrome *c* deficiency dramatically reduced HIF-1α levels (Fig. 6*A*), consistent with previous reports that mitochondria are important for hypoxic HIF-1α stabilization (40–42). Hypoxia inhibited mTOR activity up to 6 h in both wild type and cytochrome *c* null ECs, as indicated by rpS6 and 4EBP1 hypophosphorylation (Fig. 6*A*) (data not shown). eEF2 phosphorylation was also unaffected by

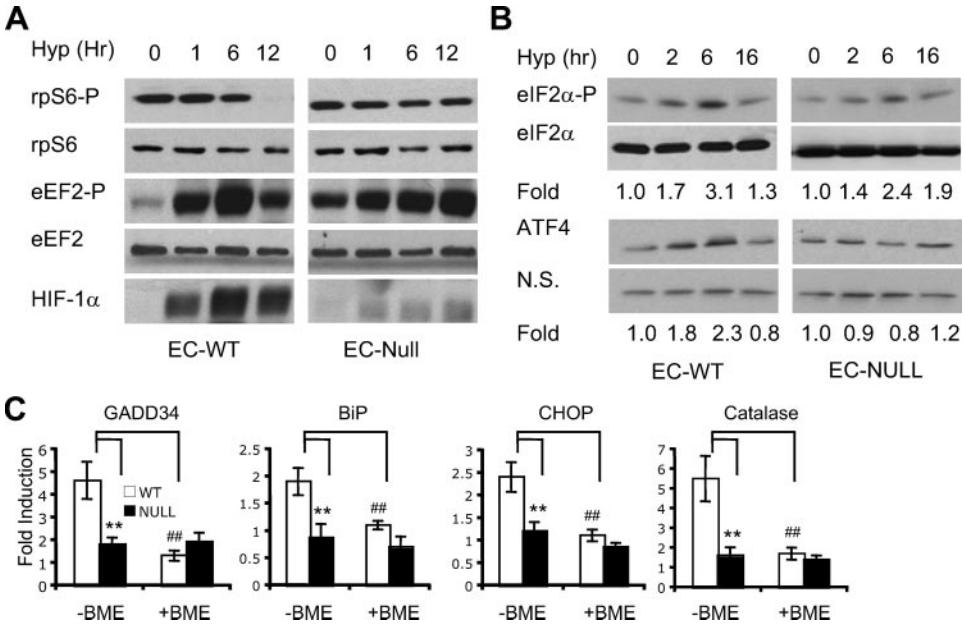

FIGURE 6. **Mitochondrial ROS activate the ISR during hypoxia.** *A* and *B*, cytochrome *c* wild type (*EC-WT*) or null (*EC-Null*) embryonic cells were exposed to 0.5% O_2 for 0–12 h. Phospho-rpS6, -eEF2, and HIF-1α proteins (*A*) and phospho-eIF2α and ATF4 proteins (*B*) were examined by Western blot. Levels of total rpS6 and eEF2 proteins (*A*) and eIF2α proteins (*B*) were analyzed for protein stability. *N.S.*, nonspecific protein band for sample loading. Increases in eIF2α phosphorylation and ATF4 protein levels compared with 0 h hypoxia are indicated. *C*, effects of cytochrome *c* mutation on hypoxic induction of catalase and ISR genes *GADD34*, *BiP*, *CHOP*, and catalase in EC cells. Cytochrome *c* wild type and null cells were exposed to 0.5% O_2 for 16 h in the presence or absence of BME (100 μM). Cells were then harvested for mRNA analysis. **, $p < 0.01$; cytochrome *c* WT *versus* null EC in the absence of BME. ##, $p < 0.01$; WT EC in the presence or absence of BME.

cytochrome *c* deficiency. Interestingly, hypoxic mTOR inhibition was significantly alleviated by cytochrome *c* deletion after 12 h (Fig. 6*A*). This difference probably results from impaired HIF-mediated REDD1 induction in cytochrome *c* null ECs and therefore reduced activation of the REDD1/TSC2/mTOR pathway in hypoxic cells (19).

Of note, cytochrome *c* mutagenesis suppressed hypoxic eIF2α phosphorylation and ATF4 protein accumulation after 6 h of 0.5% O_2 (Fig. 6*B*) as well as the induction of GADD34, BiP, and CHOP at 16 h (Fig. 6*C*). These data demonstrate that mtROS activate the ISR during hypoxia. BME pretreatment effectively decreased ER stress gene induction in wild type cells but not in cytochrome *c* null ECs (Fig. 6*C*). Interestingly, hypoxia also enhanced catalase expression, which was effectively blocked by BME and cytochrome *c* loss (Fig. 6*C*). Altogether, our data suggest that ROS, especially mtROS, play an important role in hypoxic activation of the ISR.

ISR Activation Protects Cells against O_2 and Growth Factor Withdrawal—Previous studies by Bi *et al.* have shown that $\leq$0.02% O_2 induces apoptosis within 12 h, and the PERK/eIF2α pathway is an important protective mechanism for cells experiencing anoxia (27). Since moderate hypoxia ($\geq$0.2% O_2) has been shown to affect cell survival differently from anoxia (17), we evaluated the effects of the ISR on cell survival at 0.5% O_2 using MEFs carrying knock-in alleles of eIF2α S51S (control cells) or S51A. Notably, the S51A mutation abolishes eIF2α phosphorylation caused by hypoxia, H_2O_2, and thapsigargin (Fig. 7*A*). As a consequence, downstream ISR responses, including eIF-2α-mediated global translation inhibition, selective ATF4 translation, and induction of ATF4 target genes, are abrogated by the S51A mutation.

We exposed S51S and S51A MEFs cultured in regular medium (10% FBS, 4.5 g/liter glucose) to 21 or 0.5% O_2 for 48 h. Cell viability was assessed by colony formation. Consistent with a recent report that modest hypoxia alone is not cytotoxic (17), S51S and S51A MEFs formed comparable numbers of colonies under normoxia and hypoxia (Fig. 7*B*), indicating that hypoxia resulted in only insignificant amounts of cell death (<10%) for both cell types. We then added secondary stresses by reducing glucose or serum concentrations in the culture medium to mimic cells residing in solid tumors, ischemic tissue, and stroke, where they are probably starved for growth factors and/or nutrients in addition to O_2. Glucose reduction from 4.5 g/liter to 0.2 g/liter (10% FBS) did not result in any significant cell death following 48 h of normoxia or hypoxia (Fig. 7*B*). In contrast, growth factor withdrawal significantly attenuated cell survival under 0.5% O_2. Approximately 90 and 98% cell death was detected for S51S and S51A MEFs, respectively, under low O_2 when serum was decreased from 10 to 0.5%, despite high glucose concentrations (Fig. 7*B*). Neither 2-day glucose nor serum deprivation altered eIF2α phosphorylation in S51S MEFs during normoxia (Fig. 7*B*). Therefore, in direct contrast to anoxia, hypoxia alone does not cause appreciable cell death. We concluded that growth factor availability is critical for maintaining cell viability during chronic hypoxia.

Since 48 h O_2 and serum starvation resulted in $\geq$90% death for both S51S and S51A MEFs, we examined the effect of the ISR on cellular resistance to hypoxia by limiting treatment to 24 h. As shown in Fig. 7, *D* and *E*, cell survival was enhanced by less pronounced stress (0.5% O_2, 0.5% FBS, and 4.5 g/liter glucose) for a shorter period of time. S51S cells exhibited 60% survival, as assessed by colony formation (Fig. 7, *D* and *E*). However, the eIF2α S51A mutation greatly compromised cell survival to 25% of normoxia under these combined stresses (Fig. 7, *C* and *D*), demonstrating that the ISR protects cells from low O_2 and growth factor withdrawal. Moreover, ISR activation helps to maintain cellular energy balance under low O_2. Intracellular ATP levels were lowered to ~55% of normoxic levels in S51S cells, and S51A mutation resulted in significantly lower ATP levels (Fig. 7*F*). Together, our data demonstrate that cells with a compromised ISR pathway exhibit elevated sensitivity to O_2 and growth factor deprivation. Therefore, an intact PERK/eIF2α pathway facilitates energy maintenance and cell survival during metabolic stress. However, prolonged O_2 deprivation

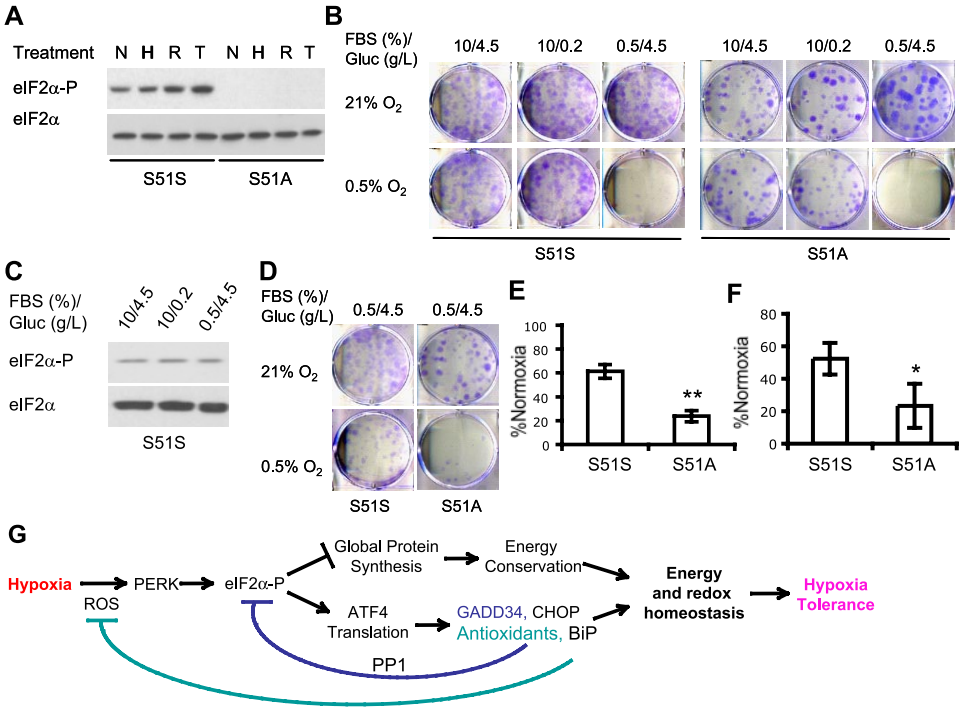

FIGURE 7. **The PERK/eIF2α pathway is critical for adaptation to low O_2 and growth factor conditions.** *A*, eIF2α S51S and S51A MEFs were exposed to 20 h of 0.5% O_2 (*H*), 1 h 20 μM H_2O_2 (*R*), or 4 h of 0.8 μM thapsigargin (*T*). eIF2α phosphorylation in total lysates was determined. *B*, eIF2α S51S or S51A MEFs were exposed to 21 or 0.5% O_2 for 48 h in medium containing full (10%) or reduced (0.5%) FBS and full (4.5 g/liter) or reduced glucose (*Gluc*) (0.2 g/liter). Cell survival was examined by colony formation in regular medium (10% FBS/4.5 g/liter glucose) under normoxia for an additional 7 days. Colonies were stained using 4% crystal violet. *C*, eIF2α phosphorylation in S51S MEFs after growing for 48 h in normoxia in regular medium (*10/4.5*), or medium containing 0.2 g/liter glucose (*10/0.2*) or 0.5% FBS (*0.5/4.5*). *D* and *E*, survival for S51S or S51A MEFs exposed to 21 or 0.5% O_2 for 24 h in serum-reduced medium containing 0.5% FBS. Shown are representative assays (*D*) and quantification of colonies (*E*) ($n = 4$). **, $p < 0.01$. *F*, intracellular ATP levels in S51S and S51A MEFs after 48 h of 21 or 0.5% O_2 in medium containing 0.5% FBS, 4.5 g/liter glucose. The numbers were corrected with normoxic ATP levels. *, $p < 0.05$. *G*, schematic diagram for hypoxic activation of the ISR and biological significance of this regulation. ROS are the signaling molecules that induce ISR during hypoxia.

(48 h) coupled with growth factor withdrawal results in cell death even if the ISR is intact.

DISCUSSION

We show here that oxidative stress inhibits mRNA translation by modulating the phosphorylation of key regulators, including 4EBP1, rpS6, eIF2α, and eEF2. Cells exposed to significant levels of exogenous H_2O_2 trigger eIF2α phosphorylation by multiple kinases and also inhibit mTOR in a dose-dependent manner through TSC2-independent mechanisms. In addition, intracellular ROS produced under hypoxic conditions play an important role in activating the PERK/eIF2α/ATF4 pathway. This response is quite specific, since hypoxic ROS do not affect mTOR and eEF2 activities. Finally, the ISR induced by PERK/eIF2α/ATF4 is adaptive and promotes cell survival during O_2 deprivation.

The mechanisms by which oxidative stress regulate the eIF2α kinases are complex and are not completely understood. Xue *et al.* (34) reported that ROS generated by TNFα signaling can activate PERK, whereas eIF2α phosphorylation induced by arsenate does not involve PERK. Here, we demonstrate that H_2O_2 promotes PERK-mediated eIF2α phosphorylation, thereby inhibiting protein synthesis. Direct activation of PERK by H_2O_2 and hypoxia was reflected in the modest but reproducible change in PERK protein mobility, which is similar to that reported for cells treated with TNFα (34). Our data also indicate that multiple eIF2α kinases, including PERK and PKR, regulate eIF2α phosphorylation in response to exogenous ROS (Fig. 4*C*). GCN2 plays a minor role at most, since H_2O_2 treatment elicited comparable changes in protein synthesis in PERK$^{-/-}$ and PERK$^{-/-}$/GCN2$^{-/-}$ DKO MEFs.

Our data demonstrate that the ISR is induced in hypoxic cells through activation of the PERK/eIF2α/ATF4 pathway. Interestingly, other regulatory pathways known to inhibit mRNA translation (mTOR and eEF2) were not affected by hypoxic ROS. These seemingly disparate effects of ROS suggest that their concentration in hypoxic cells may be insufficient to activate mTOR and eEF2 responses. This notion is supported by the observation that relatively high doses of exogenous H_2O_2 are required to exert effects on mTOR and eEF2 activity. Either the PERK/eIF2α/ATF4 pathway has a particularly low threshold for activation by ROS, or PERK is exposed to high localized ROS concentrations in the ER of hypoxic cells.

Many studies have demonstrated that hypoxic ROS are generated from the mitochondrial electron transport chain (39–41). It is also possible that ROS produced directly in the ER by ERO1 contribute to PERK activation. Oxidative protein folding occurs in the ER, which has a relatively low ratio of GSH/GSSG (1:1 to 3:1) compared with a greater than the 50:1 ratio in the cytoplasm (49). Therefore, the ER may be particularly sensitive to changes in intracellular redox status. In addition, most ER ROS are produced by ERO1 through reoxidation of protein-disulfide isomerase (26, 49), and hypoxia is known to induce the expression of ERO1α (51). Interestingly, cytochrome *c* null cells (exhibiting decreased mtROS production) partially reduce PERK/eIF2α activation, suggesting that other ROS sources are involved. However, it should be noted that a physical association between the ER and mitochondria has been demonstrated, suggesting that mtROS are readily available to ER kinases (52, 53). In contrast, mTOR and eEF2 may not be accessible to mtROS, although the 2′,7′-dichlorofluorescein diacetate assays provided in supplemental Fig. 2 suggest that H_2O_2 levels in cells exposed to 0.5% O_2 are sufficient to activate these targets.

It is noteworthy that several previous reports referred to essentially anoxic conditions (≤0.02% O_2) as "hypoxic," in contrast to the levels of O_2 (0.5%-1.5%) typically used to define hypoxia. Increasing evidence indicates that hypoxia and anoxia

elicit different cellular responses. For instance, anoxia results in rapid eIF2 inhibition and a delay in eIF4F regulation (46), whereas modest hypoxia rapidly inhibits eIF4F and gradually increases eIF2α phosphorylation (13, 31, 47). Moreover, 24 h of anoxia was sufficient to induce cell death in several reports (17, 27, 54), whereas moderate hypoxia (0.5% O_2, 48 h) does not affect cell viability (Fig. 7*A*). Secondary stresses, such as serum deprivation, were required to induce cell death during 48 h of moderate hypoxia. Thus, it is important to consider the severity and the length of O_2 deprivation when studying O_2 effects on cell metabolism and survival. The ROS-induced ISR reported here is an important prosurvival mechanism under moderate hypoxia, a situation that occurs in multiple pathophysiological conditions.

ROS are well recognized for playing dual roles as both deleterious and beneficial factors. The "two-facet" character of ROS is substantiated by growing evidence that ROS can promote ER stress, DNA, protein and lipid damage, and apoptosis but can also activate adaptive intracellular signaling pathways (36–38, 48). The effects of ROS on cellular functions are likely to depend on the location and concentration of ROS produced (26). Chronic and high doses of oxidative stress may induce cell death. However, moderate ROS levels produced during hypoxia facilitate early hypoxia tolerance by inhibiting global protein translation, conserving ATP, and inducing ATF4 target genes modulating survival (*CHOP*), protein translation (*GADD34*), and removal of oxidative stress (heme oxidase-1 and enzymes involved in glutathione metabolism) via the ISR (Fig. 7*G*) (29). It is noteworthy that NRF2, another PERK substrate (48), is activated during hypoxia (55), possibly by ROS. NRF2 activates the transcription of genes encoding detoxifying enzymes and antioxidants (48). Together, ATF4 and NRF2 target genes form a negative feedback loop to modify mRNA translation and modulate energy and redox status during hypoxia (Fig. 7*G*).

We also demonstrate that both growth factor availability and ISR activation are crucial for preventing hypoxic cell death. The protective response conferred by extrinsic growth factors against O_2 deprivation is likely to involve multiple mechanisms. Growth factor signals promote nutrient uptake and their intracellular metabolism and the maintenance of mitochondrial homeostasis (56, 57). Additionally, the ability of cells to stimulate anaerobic glycolysis in response to hypoxia depends on growth factor receptor-mediated HIF signaling (6). Our data indicate that the ISR promotes hypoxia tolerance by inducing stress genes and facilitating cellular energy and redox homeostasis. This model is supported by the demonstration that cells with a compromised ISR pathway exhibit significant sensitivity to O_2 and growth factor deprivation.

Many pathologies, such as solid tumors, ischemia, stroke, neurodegerative diseases, and inflammation, result in cellular redox imbalances. Notably, these are also associated with O_2 deprivation and/or ER stress. As a result, appropriate administration of antioxidants or free radical-generating compounds are potential therapeutic modalities for treating these diseases. For example, antioxidants inhibit tumorigenesis in three different models (45). However, proper treatment strategies can only be designed based upon improved understanding of the interactions between hypoxia and ROS.

Acknowledgments—We thank members of the Simon, Diehl, and Thompson laboratories for thoughtful discussions and critical review of the manuscript.

REFERENCES

1. Simon, M. C., and Keith, B. (2008) *Nat. Rev. Mol. Cell. Biol.* **9,** 285–296
2. Semenza, G. L. (2001) *Trends Mol. Med.* **7,** 345–350
3. Wouters, B. G., van den Beucken, T., Magagnin, M. G., Koritzinsky, M., Fels, D., and Koumenis, C. (2005) *Semin. Cell Dev. Biol.* **16,** 487–501
4. Brahimi-Horn, M. C., Chiche, J., and Pouyssegur, J. (2007) *Curr. Opin. Cell Biol.* **19,** 223–229
5. Cai, S. L., Tee, A. R., Short, J. D., Bergeron, J. M., Kim, J., Shen, J., Guo, R., Johnson, C. L., Kiguchi, K., and Walker, C. L. (2006) *J. Cell Biol.* **173,** 279–289
6. Lum, J. J., Bui, T., Gruber, M., Gordan, J. D., DeBerardinis, R. J., Covello, K. L., Simon, M. C., and Thompson, C. B. (2007) *Genes Dev.* **21,** 1037–1049
7. Giaccia, A., Siim, B. G., and Johnson, R. S. (2003) *Nat. Rev. Drug Discov.* **2,** 803–811
8. Hu, C. J., Wang, L. Y., Chodosh, L. A., Keith, B., and Simon, M. C. (2003) *Mol. Cell. Biol.* **23,** 9361–9374
9. Kim, J. W., and Dang, C. V. (2006) *Cancer Res.* **66,** 8927–8930
10. Papandreou, I., Cairns, R. A., Fontana, L., Lim, A. L., and Denko, N. C. (2006) *Cell Metab.* **3,** 187–197
11. Kaelin, W. G., Jr. (2002) *Genes Dev.* **16,** 1441–1445
12. Kim, J. W., Tchernyshyov, I., Semenza, G. L., and Dang, C. V. (2006) *Cell Metab.* **3,** 177–185
13. Liu, L., Cash, T. P., Jones, R. G., Keith, B., Thompson, C. B., and Simon, M. C. (2006) *Mol. Cell* **21,** 521–531
14. Koumenis, C., and Wouters, B. G. (2006) *Mol. Cancer Res.* **4,** 423–436
15. DeYoung, M. P., Horak, P., Sofer, A., Sgroi, D., and Ellisen, L. W. (2008) *Genes Dev.* **22,** 239–251
16. Heacock, C. S., and Sutherland, R. M. (1986) *Int. J. Radiat. Oncol. Biol. Phys.* **12,** 1287–1290
17. Koritzinsky, M., Rouschop, K. M., van den Beucken, T., Magagnin, M. G., Savelkouls, K., Lambin, P., and Wouters, B. G. (2007) *Radiother. Oncol.* **83,** 353–361
18. Koumenis, C., Naczki, C., Koritzinsky, M., Rastani, S., Diehl, A., Sonenberg, N., Koromilas, A., and Wouters, B. G. (2002) *Mol. Cell. Biol.* **22,** 7405–7416
19. Brugarolas, J., Lei, K., Hurley, R. L., Manning, B. D., Reiling, J. H., Hafen, E., Witters, L. A., Ellisen, L. W., and Kaelin, W. G., Jr. (2004) *Genes Dev.* **18,** 2893–2904
20. Reiling, J. H., and Hafen, E. (2004) *Genes Dev.* **18,** 2879–2892
21. Bernardi, R., Guernah, I., Jin, D., Grisendi, S., Alimonti, A., Teruya-Feldstein, J., Cordon-Cardo, C., Simon, M. C., Rafii, S., and Pandolfi, P. P. (2006) *Nature* **442,** 779–785
22. Blais, J. D., Addison, C. L., Edge, R., Falls, T., Zhao, H., Wary, K., Koumenis, C., Harding, H. P., Ron, D., Holcik, M., and Bell, J. C. (2006) *Mol. Cell. Biol.* **26,** 9517–9532
23. Connolly, E., Braunstein, S., Formenti, S., and Schneider, R. J. (2006) *Mol. Cell. Biol.* **26,** 3955–3965
24. Blais, J. D., Filipenko, V., Bi, M., Harding, H. P., Ron, D., Koumenis, C., Wouters, B. G., and Bell, J. C. (2004) *Mol. Cell. Biol.* **24,** 7469–7482
25. Hamanaka, R. B., Bennett, B. S., Cullinan, S. B., and Diehl, J. A. (2005) *Mol. Biol. Cell* **16,** 5493–5501
26. Malhotra, J. D., and Kaufman, R. J. (2007) *Antioxid. Redox Signal.* **9,** 2277–2293
27. Bi, M., Naczki, C., Koritzinsky, M., Fels, D., Blais, J., Hu, N., Harding, H., Novoa, I., Varia, M., Raleigh, J., Scheuner, D., Kaufman, R. J., Bell, J., Ron, D., Wouters, B. G., and Koumenis, C. (2005) *EMBO J.* **24,** 3470–3481
28. Marciniak, S. J., Garcia-Bonilla, L., Hu, J., Harding, H. P., and Ron, D. (2006) *J. Cell Biol.* **172,** 201–209
29. Harding, H. P., Zhang, Y., Zeng, H., Novoa, I., Lu, P. D., Calfon, M., Sadri, N., Yun, C., Popko, B., Paules, R., Stojdl, D. F., Bell, J. C., Hettmann, T., Leiden, J. M., and Ron, D. (2003) *Mol. Cell* **11,** 619–633

30. Novoa, I., Zeng, H., Harding, H. P., and Ron, D. (2001) *J. Cell Biol.* **153,** 1011–1022
31. Arsham, A. M., Howell, J. J., and Simon, M. C. (2003) *J. Biol. Chem.* **278,** 29655–29660
32. Lu, P. D., Jousse, C., Marciniak, S. J., Zhang, Y., Novoa, I., Scheuner, D., Kaufman, R. J., Ron, D., and Harding, H. P. (2004) *EMBO J.* **23,** 169–179
33. Patel, J., McLeod, L. E., Vries, R. G., Flynn, A., Wang, X., and Proud, C. G. (2002) *Eur. J. Biochem.* **269,** 3076–3085
34. Xue, X., Piao, J. H., Nakajima, A., Sakon-Komazawa, S., Kojima, Y., Mori, K., Yagita, H., Okumura, K., Harding, H., and Nakano, H. (2005) *J. Biol. Chem.* **280,** 33917–33925
35. Lu, L., Han, A. P., and Chen, J. J. (2001) *Mol. Cell. Biol.* **21,** 7971–7980
36. Finkel, T. (2001) *IUBMB Life* **52,** 3–6
37. Genestra, M. (2007) *Cell. Signal.* **19,** 1807–1819
38. Rhee, S. G. (1999) *Exp. Mol. Med.* **31,** 53–59
39. Chandel, N. S., Maltepe, E., Goldwasser, E., Mathieu, C. E., Simon, M. C., and Schumacker, P. T. (1998) *Proc. Natl. Acad. Sci. U. S. A.* **95,** 11715–11720
40. Guzy, R. D., Hoyos, B., Robin, E., Chen, H., Liu, L., Mansfield, K. D., Simon, M. C., Hammerling, U., and Schumacker, P. T. (2005) *Cell Metab.* **1,** 401–408
41. Mansfield, K. D., Guzy, R. D., Pan, Y., Young, R. M., Cash, T. P., Schumacker, P. T., and Simon, M. C. (2005) *Cell Metab.* **1,** 393–399
42. Brunelle, J. K., Bell, E. L., Quesada, N. M., Vercauteren, K., Tiranti, V., Zeviani, M., Scarpulla, R. C., and Chandel, N. S. (2005) *Cell Metab.* **1,** 409–414
43. Duranteau, J., Chandel, N. S., Kulisz, A., Shao, Z., and Schumacker, P. T. (1998) *J. Biol. Chem.* **273,** 11619–11624
44. Scheuner, D., Song, B., McEwen, E., Liu, C., Laybutt, R., Gillespie, P., Saunders, T., Bonner-Weir, S., and Kaufman, R. J. (2001) *Mol. Cell* **7,** 1165–1176
45. Gao, P., Zhang, H., Dinavahi, R., Li, F., Xiang, Y., Raman, V., Bhujwalla, Z. M., Felsher, D. W., Cheng, L., Pevsner, J., Lee, L. A., Semenza, G. L., and Dang, C. V. (2007) *Cancer Cell* **12,** 230–238
46. Koritzinsky, M., Magagnin, M. G., van den Beucken, T., Seigneuric, R., Savelkouls, K., Dostie, J., Pyronnet, S., Kaufman, R. J., Weppler, S. A., Voncken, J. W., Lambin, P., Koumenis, C., Sonenberg, N., and Wouters, B. G. (2006) *EMBO J.* **25,** 1114–1125
47. Magagnin, M. G., Koritzinsky, M., and Wouters, B. G. (2006) *Drug Resist. Updat.* **9,** 185–197
48. Cullinan, S. B., and Diehl, J. A. (2004) *J. Biol. Chem.* **279,** 20108–20117
49. Gorlach, A., Klappa, P., and Kietzmann, T. (2006) *Antioxid. Redox Signal.* **8,** 1391–1418
50. Marciniak, S. J., Yun, C. Y., Oyadomari, S., Novoa, I., Zhang, Y., Jungreis, R., Nagata, K., Harding, H. P., and Ron, D. (2004) *Genes Dev.* **18,** 3066–3077
51. Gess, B., Hofbauer, K. H., Wenger, R. H., Lohaus, C., Meyer, H. E., and Kurtz, A. (2003) *Eur. J. Biochem.* **270,** 2228–2235
52. Perkins, G., Renken, C., Martone, M. E., Young, S. J., Ellisman, M., and Frey, T. (1997) *J. Struct. Biol.* **119,** 260–272
53. Csordas, G., Renken, C., Varnai, P., Walter, L., Weaver, D., Buttle, K. F., Balla, T., Mannella, C. A., and Hajnoczky, G. (2006) *J. Cell Biol.* **174,** 915–921
54. Papandreou, I., Krishna, C., Kaper, F., Cai, D., Giaccia, A. J., and Denko, N. C. (2005) *Cancer Res.* **65,** 3171–3178
55. Kim, Y. J., Ahn, J. Y., Liang, P., Ip, C., Zhang, Y., and Park, Y. M. (2007) *Cancer Res.* **67,** 546–554
56. Edinger, A. L., and Thompson, C. B. (2002) *Mol. Biol. Cell* **13,** 2276–2288
57. Vander Heiden, M. G., Plas, D. R., Rathmell, J. C., Fox, C. J., Harris, M. H., and Thompson, C. B. (2001) *Mol. Cell. Biol.* **21,** 5899–5912